Macromolecules
ARTICLE

Macromolecules **2009**, *42*, 8781–8793 **8781**
DOI: 10.1021/ma901587j

Ion-Induced Stretching of Low Generation Dendronized Polymers with Crown Ether Branching Units

Alexander Ossenbach,[‡] Heinz Rüegger,[§] Afang Zhang,*[,‡] Karl Fischer,[†] A. Dieter Schlüter,[‡] and Manfred Schmidt*[,†]

[†]*Institute of Physical Chemistry, University of Mainz, Jakob-Welder-Weg 11, 55099 Mainz, Germany,* [‡]*Department of Materials, Institute of Polymers, ETH Zurich, Wolfgang-Pauli-Str. 10, HCI J541, 8093 Switzerland, and* [§]*Laboratory for Inorganic Chemistry, ETH Zurich, Wolfgang-Pauli-Str. 10, HCI D117, 8093 Switzerland*

Received July 20, 2009; Revised Manuscript Received August 29, 2009

ABSTRACT: Synthesis of the first (G1) and second generation (G2) dendronized macromonomers **MG1** and **MG2** with the dibenzo-24-crown-8 moiety as branching unit is reported. The corresponding dendronized polymers, the polymethacrylates **PG1** and **PG2**, were synthesized by free radical polymerization using AIBN as initiator at 60−80 °C. Static and dynamic light scattering revealed a significant chain expansion upon complexation of these polymers' crown ether side chains with K^+ ions. It is concluded that electrostatic repulsion does not significantly contribute to the chain expansion because of excessive counterion binding even well below the Manning limit, as evidenced by ^{19}F NMR and $^{1}H-^{19}F$ NOE experiments. Rather, the conformational change of the crown ether moieties upon K^+-ion binding plus the short-range interaction between ion pairs formed along the chain cause the observed significant increase in chain stiffness in terms of the Kuhn statistical segment length, l_k, from $l_k = 8$ to 19 nm and from $l_k = 19$ to 45 nm for the **PG1** and **PG2** polymers, respectively. At full KPF_6 loading, the effect is as large as to triple the molar mass of the side chains, as evidenced by the similar values of the Kuhn statistical segment length of the fully complexed **PG1** as compared with the noncomplexed **PG2** sample. It is thus demonstrated that steric repulsion induced by host−guest interactions is well suitable to control the conformation of polymers with densely grafted side chains.

Introduction

Dendronized polymers have received considerable attention because of their unusual, highly branched yet overall linear molecular structure and several potential applications. For reviews, see refs 1−3. So far, the focus of research has been on the increase in the main chain stiffness with increasing side chain generation or molar mass, on the effect of peripheral functional groups, and on the nature of the polymer backbone. The nature of the dendrons themselves was of less importance, although quite a few successful chemical pathways for their construction were developed. Up to now, they basically served to fill the space between backbone and surface functional groups to create the polymers' thick, sausage-like shape and concomitantly control the main chain stiffness as a function of architecture and generation of the dendron side chains.[4−6] Also, stimulus-responsive dendronized polymers were reported in solution[7] and in bulk.[8,9]

Crown ethers (CEs) are powerful and selective hosts for various guest molecules and ions[10] and in this capacity were incorporated into a manifold of substrates including dendrons[11−14] and dendrimers.[15−20] They were also widely used in polymer chemistry,[21−24] for example, to induce backbone helicity through host/guest interaction.[25−27] In a recent case, Stoddart et al. reported that a polyacetylene (DP_w = 33) and a polystyrene (DP_w = 650) with pendant CEs can be turned into supramolecular dendronized polymers if dendrons are "grafted" to these backbones through ionic interactions between the pendant CEs and the dendrons' focal point ammonium ions.[28] Acid−base switchable conformations (rodlike upon complexation, coil-like upon decomplexation) were postulated, but unfortunately, the light scattering experiments presented do not support this claim.[29] Nevertheless, this publication points toward an interesting possibility for CE-derived dendronized polymers, namely, to switch their backbone conformation and rigidity upon the addition/removal of proper guest compounds.

A few years back, we started to explore whether the interior branches of dendronized polymers could be given a function and considered CE-based dendrons to represent an interesting starting point. Such dendrons should provide an easy handle to alter the persistence length of the corresponding dendronized polymers by exploiting the crowns' capacity to "load" and "unload" organic compounds, metal ions, and protons. In the present work, the synthesis and single crystal X-ray diffractometric analysis of a new branching unit in dendrimer chemistry based on the dibenzo 24-crown-8 moiety as well as the synthesis of the corresponding first (G1) and second generation (G2) dendronized polymethacrylates **PG1** and **PG2** (Figure 1) are reported. The change of the backbone conformation of polymers **PG1** and **PG2** upon complex formation with potassium ions was explored by static and dynamic light scattering.

Results and Discussion

Synthesis and Analysis of Dendrons and Macromonomers. The synthesis of **MG1** is delineated in Scheme 1. The key compound **3**, which is the branching unit for the CE dendron construction, was synthesized from the known compounds **1** and **2** with KPF_6 as the template under pseudo-high dilution conditions, meaning that the reactants together with the

*Corresponding author. Fax: (+41)44-6331395. E-mail: afang.zhang@mat.ethz.ch (A.Z.); mschmidt@uni-mainz.de (M.S).

Published on Web 09/28/2009

template were added dropwise to a warm suspension of K_2CO_3. This Williamson etherification reaction afforded the trifunctional dibenzo-24-crown-8 **3** on the 10 g scale in yields of 78%. The reduction of the aldehyde in **3** was done with $NaBH_4$ and cleanly afforded the benzyl alcohol **4**, leaving the esters untouched if the reaction was carried out in a 1:1 mixture of THF and methanol at room temperature. The use of ethanol as a more common solvent for $NaBH_4$ proved to be disadvantageous because transesterification occurs. The THF/MeOH solvent mixture avoided ester reduction and afforded the desired product within 2 h in a yield of 95%. To convert it into the G1 macromonomer **MG1**, methacryloyl chloride (MAC) was reacted with the alcohol function.

The G2 macromonomer **MG2** was synthesized as shown in Scheme 2. The aldehyde function of compound **3** was protected with 1,3-dihydroxypropane as an O,O acetal (**5**).

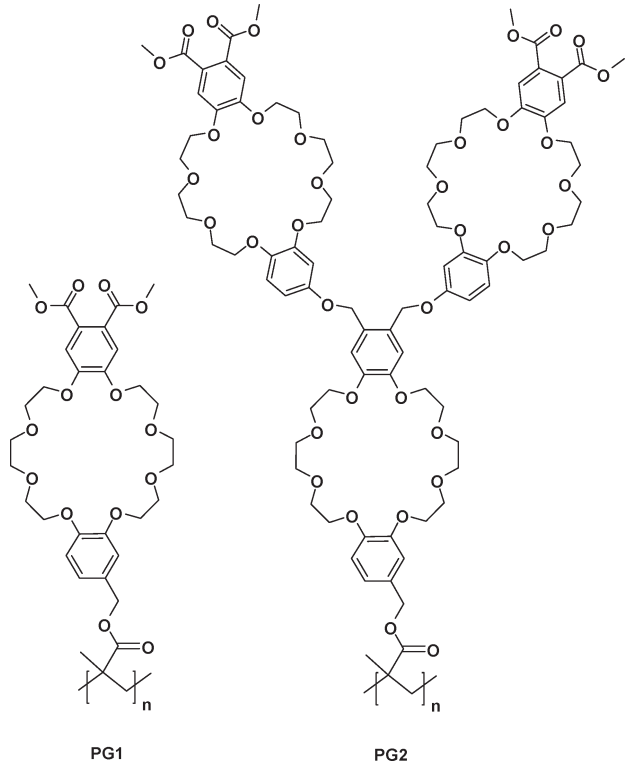

Figure 1. Chemical structures of dibenzo-24-crown-8 dendronized polymethacrylates **PG1** and **PG2** synthesized.

The ester functions of **5** were then converted to benzyl alcohol **6** with di-isobutylaluminium hydride (DIBAL-H). Its conversion into the two-fold benzyl chloride **7** was achieved by the reaction with thionyl chloride in dry dichloromethane (DCM) below 0 °C. The acetal was in situ cleaved during aqueous workup. Phenol **8** was obtained from **3** under Baeyer−Villiger rearrangement/oxidation conditions with H_2O_2 in MeOH. Etherification of phenol **8** with benzyl dichloride **7** afforded G2 dendron **9**. By reduction of **9** with $NaBH_4$, followed by reaction with MAC, G2 macromonomer **MG2** was prepared. All new compounds have been prepared and purified to give highly pure substances deduced by NMR spectroscopy and elemental analysis. In particular, the macromonomers **MG1** and **MG2** had to be highly pure before starting polymerizations.

Additionally a single crystal of **3** was obtained from methanol by slow evaporation. The molecular structure and the packing behavior are shown in Figure 2. Compound

Scheme 2. Synthesis of the G2 Crown Ether Dendron 9 and Its Respective Monomer MG2[a]

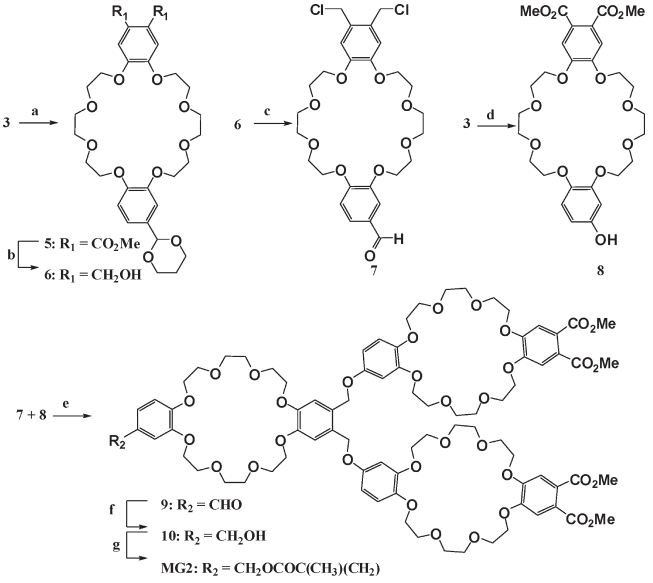

[a] Reagents and conditions: (a) 1,3-dihydroxypropane, *p*-TsOH, benzene, 16 h, reflux, 99%; (b) DIBAL-H, THF, 2 h, room temp, 94%; (c) $SOCl_2$, DMF, DCM, 0 °C, 2 h, 83%; (d) H_2O_2, H_2SO_4, MeOH, 60°C for 1 h, room temp 15 h, 59%; (e) Cs_2CO_3, KI, DMF, 60 °C, 48 h, 76%; (f) $NaBH_4$, THF/MeOH 1:1, room temp, 3 h, 99%; (g) MAC, LiBr, TEA, THF, room temp, 24 h, 75%.

Scheme 1. Synthesis of Crown Ether Dendron 3 and the Respective Macromonomer MG1[a]

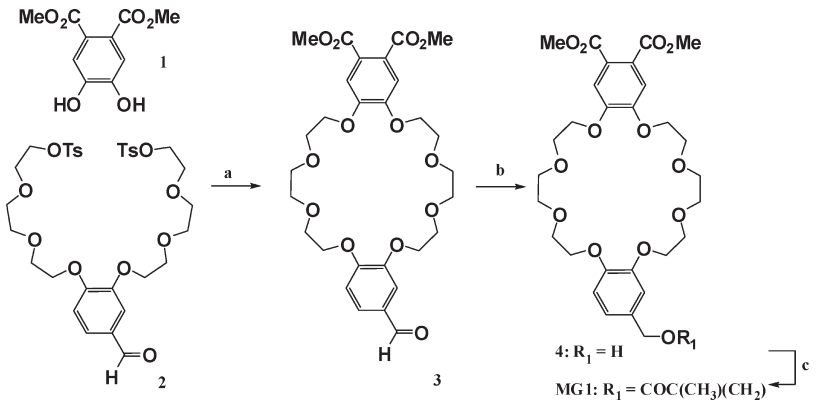

[a] Reagents and conditions: (a) K_2CO_3, KPF_6, CH_3CN, 65 °C, 24 h, 78%; (b) $NaBH_4$, THF/MeOH, room temp, 3 h, 95%; (c) MAC, LiBr, TEA, THF, room temp, 24 h, 75%.

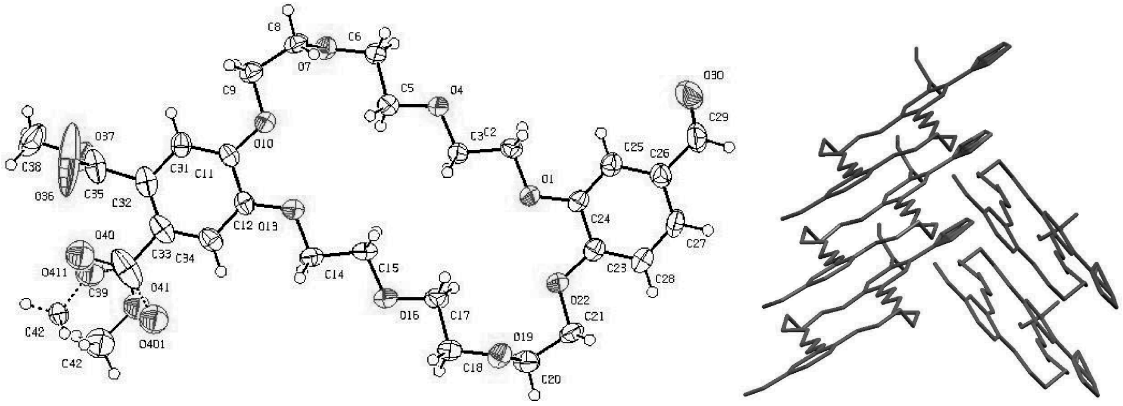

Figure 2. Single crystal X-ray diffraction molecular structure of **3** (left) and packing motif of **3** in the crystal (right).

Table 1. Polymerization Results of MG1 and MG2[a]

entry	m (mg)	c (g/L)	AIBN wt %	temp (°C)	t (h)	yield %	M_w (10^6 g/mol)	M_n (10^6 g/mol)	PDI	M_w (LS) (10^6 g/mol)	T_g (°C)
1 (**PG1**)	200	1	0.2	60	16	97	1.81	0.89	2.0	2.89	56
2 (**PG2**)	505	1.68	0.2	75	40	41	0.5	0.25	2.0	0.72	
3 (**PG2**)	510	2.04	0.2	80	48	57	3.48	1.35	2.6	4.73	51

[a] Polymerizations furnishing **PG1** and **PG2** were carried out in DMF with AIBN as initiator for 8−48 h. Molar masses determined in DMF (1% LiBr) at 45 °C against PMMA standard. M_w (LS) determined in CH_3CN with 1×10^{-2} mol/L PPh_4Br.

3 crystallized in a $Pca2_1$ space group, and the cavity has a diameter of 4.5 × 9.4 Å (distance O4−C15 and O22−O10, respectively). One of the ester groups attached is not resolved because of two possible orientations parallel to the aromatic ring, whereas the other one is perpendicular to the aromatic rings. The aromatic rings are in one plane. The orthorhombic crystal lattice contains one methanol and one water molecule per CE (not shown). Interestingly, neither the methanol nor the water is situated in the CE cavity; rather, they are positioned close to the ester.

The crystal structure of the corresponding parent dibenzo-24-crown-8 has a monoclinic crystal lattice with a $P2_1/c$ space group. In contrast with the asymmetric **3**, the symmetric DB24C8 shows a chairlike conformation in which the aromatic rings are coplanar to each other but are not in the same plane.[30]

Polymerization and Characterization. The polymerization reactions were carried out on the 200 mg scale for **MG1** and the 500 mg scale for **MG2** in highly concentrated DMF solutions (required to achieve high degrees of polymerization for bulky monomers like polymacromonomers or dendrons) at 60−80 °C with AIBN as the initiator. The results are summarized in Table 1. The relative molar masses and the molar mass distributions were estimated by gel permeation chromatography using standard calibration versus a PMMA standard. All elution curves were monomodal. Absolute molar masses, as determined by light scattering, are also included in Table 1. The polymerization conditions on the first generation with 60 °C and a monomer concentration of 1 g/L gave satisfying results with $M_w = 2.89 \times 10^6$ g/mol, whereas for the polymerization of **MG2**, higher concentrations and elevated temperatures were applied to achieve the high-molecular-weight polymer **PG2** with $M_w = 4.73 \times 10^6$ g/mol (entry 3). It should be noted that polymerization at higher temperatures occasionally led to gelation of significant parts of the product; These gels were not soluble in common organic solvents.

The static and dynamic light scattering results of all polymer samples dissolved in pure acetonitrile showed an anomalous behavior: The reduced scattering intensity Kc/R_θ decreased with increasing scattering vector, q (Figure 3b), which would result in an unphysical negative radius of

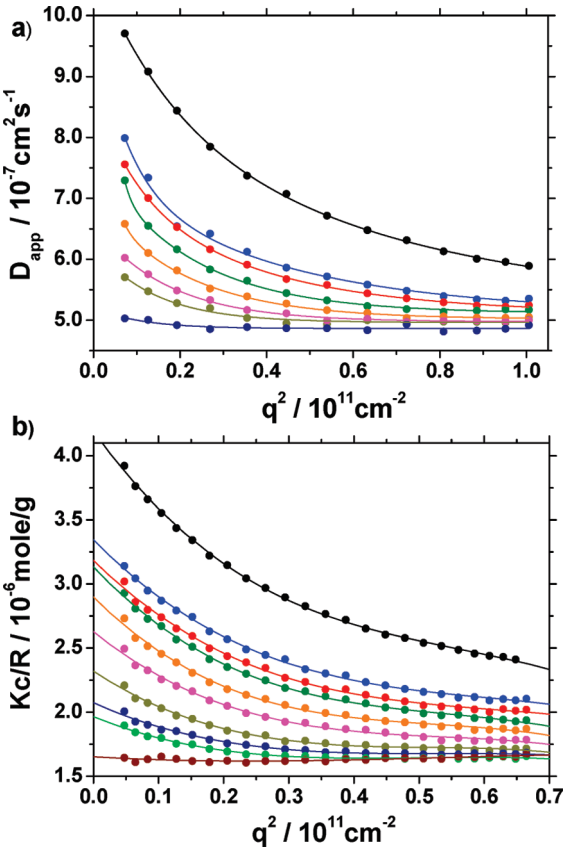

Figure 3. DLS and SLS results for sample **PG2 entry 2** measured in acetonitrile with no added salt: (a) Apparent diffusion coefficient derived from the fast relaxation $D_{app,f}$ versus q^2 (concentrations from top to bottom 1.00, 0.598, 0.475, 0.354, 0.233, 0.1669, 0.1095, 0.0404 g/L) and (b) reduced scattering intensity versus q^2 for different concentration (concentration from top to bottom 1.00, 0.86, 0.73, 0.62, 0.50, 0.38, 0.25, 0.17, 0.13, 0.04 g/L).

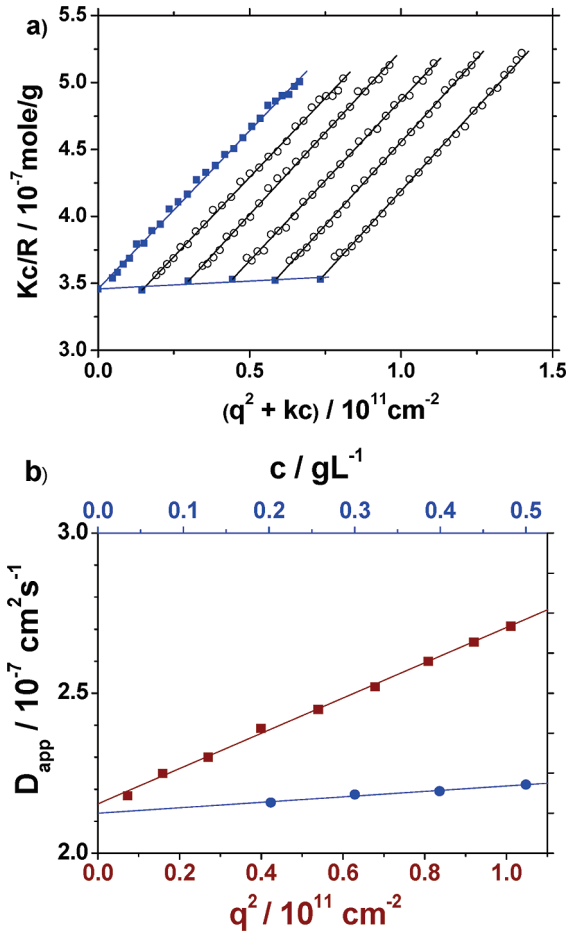

Figure 4. (a) Static Zimm plot and (b) D_{app} versus q^2 (c = 0.40 g/L, brown squares, lower scale) and D_{app} ($q = 0$) versus concentration (blue circles, upper scale) for sample **PG1 entry 1** in acetonitrile containing 1×10^{-2} M PPh_4Br. $M_w = 2.89 \times 10^6$ g/mol, R_g = 45.2 nm, R_h = 27.9 nm.

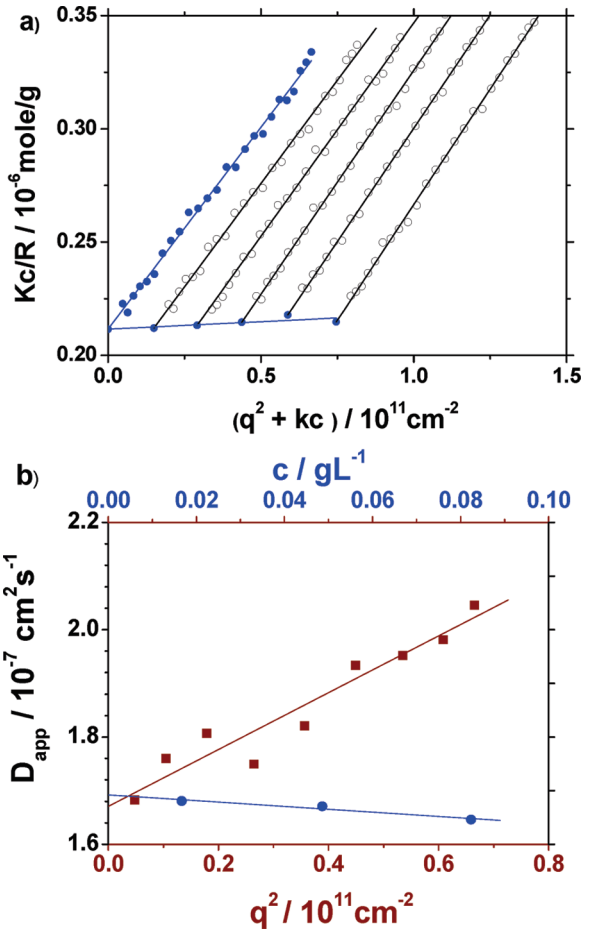

Figure 5. (a) Static Zimm plot and (b) D_{app} versus q^2 (red squares, lower scale, c = 0.048 g/L) and D_{app} ($q = 0$) versus concentration (blue circles, upper scale) of sample **PG2 entry 3** in acetonitrile containing 10^{-2} M PPh_4Br. $M_w = 4.73\ 10^6$ g/mol, R_g = 50.2 nm, R_h = 35.1 nm.

gyration. Concomitantly, the correlation functions exhibit a bimodal decay. The slow decay scales with q^2 and leads to a hydrodynamic radius of $R_h = 100$ nm, which is much larger than expected for single polymer chains. The fast mode shows an anomalous behavior because the apparent diffusion coefficient derived from the measured relaxation time divided by q^2 decreases with increasing q^2, as shown in Figure 3a.

Such anomalies are known to occur in polyelectrolyte solutions[31] and indicate that during the synthesis some cations are already complexed by the CE groups. Only polymers with a few charges were observed to show such anomalies, particularly in organic solvents with low dielectric constant that originate from strong intermolecular electrostatic interaction.[32]

This hypothesis is corroborated by the fact that normal Zimm plots and DLS measurements (no slow modes) could be obtained if monovalent salts such as KPF_6 or PPh_4Br were added to the acetonitrile solutions. To determine the molar mass and the bare chain dimensions (i.e., without or with a few cation/CE inclusion complexes), measurements were conducted in 10^{-2} M PPh_4Br because the PPh_4 cation is too bulky to form an inclusion complex. The results are shown in Figures 4 and 5 for the samples from Table 1 **entries 1** and **3** and are summarized in Table 2. The second virial coefficients, A_2, are small, indicating a moderate-to-poor solvent quality.

Monomer Complexation with K^+ Ions. CEs are known to form complexes with different cationic species. The stability and the conformation of the host−guest system depend on several factors, such as cavity size, polarity of the solvent, and so on. NMR techniques are frequently used to determine, for example, stability constants, complex stoichiometry, and microstructure in the solid state.[33−35] Both the G1 macromonomer **MG1** and the G2 dendron **9** were complexed with KPF_6 in acetonitrile. The interaction of the cation with the CE ring is observed by an up- or downfield shift of the corresponding signals of either the ethylene protons or the aromatic protons. The ^{1}H NMR chemical shifts upon complexation with potassium ions indicate a thermodynamically but not kinetically stable complex formation for both **MG1** and **9** (Figures 6 and 7). The protons H1 and H1′ (in **MG1**) have different chemical shifts because of the asymmetry of the molecule, even in the uncomplexed form. This difference can be resolved in high-resolution 700 MHz ^{1}H NMR for the noncomplexed species. The assignment of the H1 signals in Figure 6 is tentative. In **9**, all four peripheral aromatic protons are not chemically equivalent, although in the uncomplexed form, only two can be differentiated (Figure 6, only H1 and H1′ are assigned for **9**). For a qualitative estimation of the complex stoichiometry, **MG1** and **9** were titrated with KPF_6 in a ^{1}H NMR series (Figures 6 and 7).

The titration curve of the chemical shifts of **MG1** reaches a maximum at a 1:1 (CE/metal ion) stoichiometry upon complexation with potassium ions (Figure 7a). Because of the

Table 2. Summary of Static and Dynamic Light Scattering Results for Polymer Entries 1-3

entry	salt (1 10^{-2} M)	M_w (LS) (10^6 g/mol)	A_2 (10^{-5} cm^3/g^2)	R_g (nm)	R_h (nm)	L_w (nm)	l_k (nm)[a]	d (nm)[b]
1 (**PG1**)	PPh_4Br	2.89	3.5	45.2	27.9	1100	8 ± 1	3
	KPF_6	2.60	6.5	72.7	36.8	980	19 ± 2	3
2 (**PG2**)	PPh_4Br	0.72	2.8	20.4	12.8	104	19 ± 2	6
	KPF_6	0.68	9.1	27.8	15.2	98	45 ± 5	6
3 (**PG2**)	PPh_4Br	4.73	3.0	50.2	35.1	680	19 ± 2	6
	KPF_6	4.62	−9.0	84.0	48.9	670	45 ± 5	6

[a] Kuhn length. [b] Assumed thickness of the polymer.

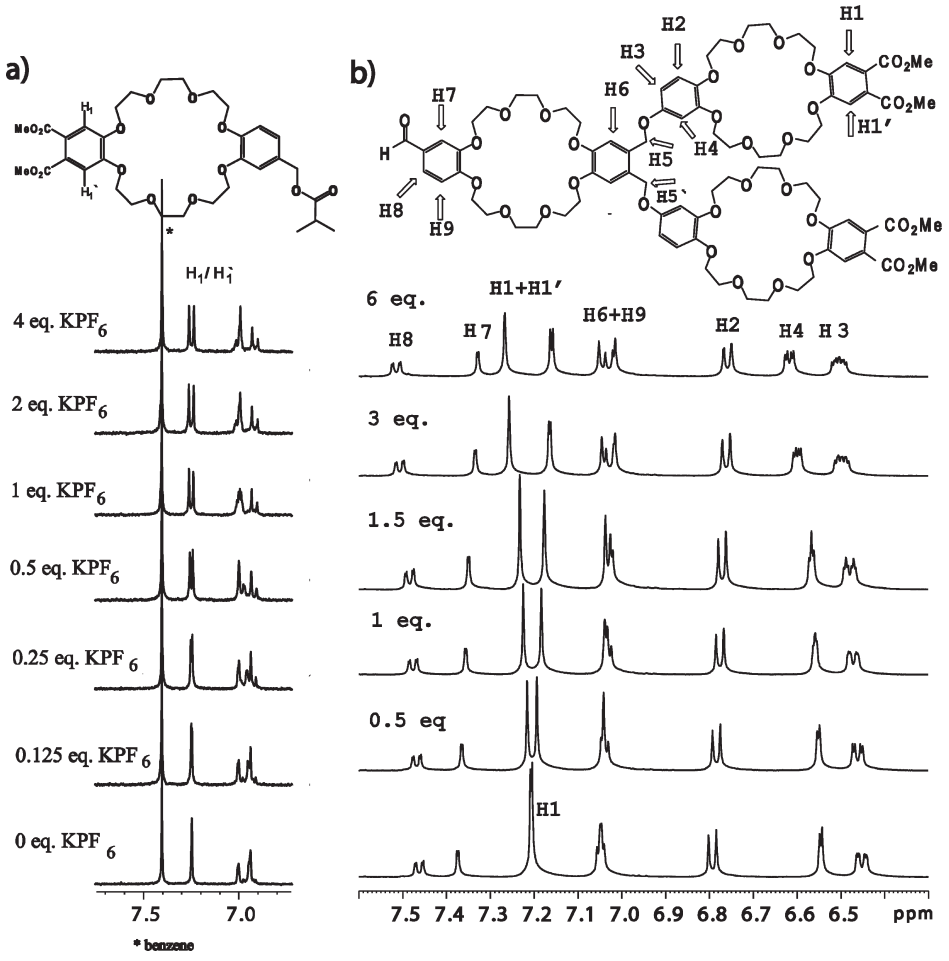

Figure 6. Aromatic region of ^{1}H NMR titration series (300 MHz, CD_3CN) of (a) **MG1** with KPF_6 ([CE] + [KPF_6] = const. = 7.55×10^{-3} mol/L) and (b) **9** ([CE] = const. = 1.93×10^{-3} mol/L). Benzene was used as internal standard in the **MG1** series.

more restricted flexibility of the CE ring, the differences in the chemical shifts of proton H1 and H1′ become more pronounced. To demonstrate that the addition of salt does not influence the chemical shifts possibly caused by changes in ionic strength, solvent quality, and so on, benzene was utilized as an internal standard in the KPF_6 titration. The chemical shift of the benzene protons was not influenced by the addition of salt.

The aromatic signals of **9** of the ^{1}H NMR experiments are shown in Figure 6b. All four protons of the H1 series can be distinguished in the spectrum of the fully complexed **9**. Also, the signal of the benzylic protons H5 (not shown) separates into two signals upon complexation with KPF_6. These signals originate from each benzylic linker. The titration curve of H1 in **9** (signal shifting from 7.1 to 7.265 ppm) shows the formation of a 1:3 (CE/metal) complex (Figure 7b) within experimental error.

Complex Formation of the Polymers with K^+. The aromatic ^{1}H NMR signals of **PG1** and **PG2** with and without an excess of KPF_6 in CD_3CN are shown in Figure 8. For **PG1**, upon complexation with KPF_6, the aromatic signal of H1/H1′ separate again into two signals, as already observed in the monomer. There is a clear shift of every signal observed in the ^{1}H NMR spectrum, indicating an interaction of the CE units of the polymer with the potassium.

Upon complexation of **PG2** with an excess of KPF_6, the signals of the H1 series separate into two signals, one shifted downfield and the other shifted upfield.

The signal of proton H6 is shifted downfield and overlaps with one of the H1 signals. The obvious shift of all aromatic protons suggests that most of the CE moieties are interacting with potassium ions. Unfortunately, broad signals, small relative changes in the chemical shifts, and overlapping signals prohibit a clear analysis of the ^{1}H NMR titrations. Also, a cooperative effect (e.g., 11% potassium per CE induces a relative change of the signal at 4.115 ppm of 60% for **PG1**) on the chemical shifts makes it impossible to determine the fraction of complexed potassium. (See the

Supporting Information.) Control experiments on the uncomplexed polymers revealed no concentration dependence of the chemical shifts in the concentration regime investigated.

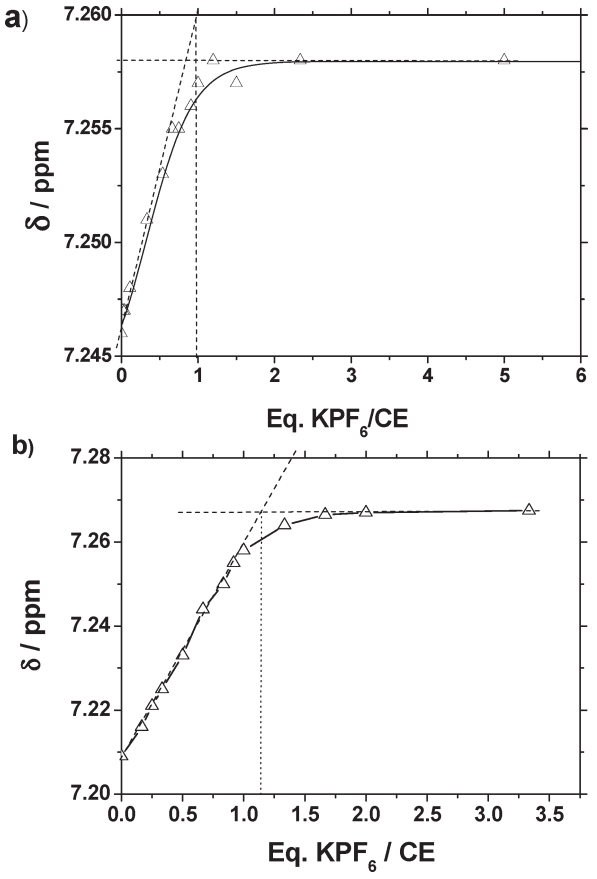

Figure 7. ^{1}H NMR chemical shift titration of the aromatic proton H1 in (a) **MG1** ([CE] + [KPF_6] = const. = 7.55×10^{-3} mol/L) and (b) **9** ([CE] = const. = 1.93×10^{-3} mol/L). The dotted line indicates the stoichiometry of the formed complex.

Alternatively, a shift in the ^{19}F NMR spectra with increasing ratios of potassium content was observed with KPF_6 originating from counterion binding/condensation. This does not occur during the complexation of **MG1** or **9**. Because the interchange of the K^+-ion-loaded CE side chains and PF_6^- is too fast to be resolved on the NMR time scale of a 500 MHz instrument, an averaged signal δ_{av} is observed and given by

$$\delta_{av} = x \cdot \delta_{bound} + y \cdot \delta_{free}$$

where δ_{bound} is the chemical shift of the bound or condensed PF_6^- and δ_{free} is the chemical shift of free PF_6^-.

To estimate δ_{bound}, it is assumed that at a high excess of potassium ions ($X_{KPF6} > 0.8$) all CE moieties carry a K^+ ion and each bound K^+ ion forms an ion pair with the PF_6^- counterions; that is, this approach neglects the amount of free K^+ ions along the polymer chain and underestimates the fraction of K^+ ions complexed by the CE moieties, accordingly. The solid lines in Figure 9a,b then constitute the theoretical curves for infinitely large complex constants and yield the chemical shift for pure complexes at $X_{KPF6} = 0$ as $\delta_{bound} = 72.277$ ppm for **PG1** and $\delta_{bound} = 72.006$ ppm for **PG2**. The ratio

$$\frac{\delta_{av} - \delta_{free}}{\delta_{bound} - \delta_{free}} = \frac{[PF_6^-]_{bound}}{[PF_6^-]_{total}}$$

represents the part of bound PF_6^- over the total amount of PF_6^-. From that ratio, the number of PF_6^- ions bound per CE may be calculated and is shown in Figure 10a,b.

The interaction of PF_6^- ions with the CE moieties is mediated by the complexation of K^+ ions by counterion binding or Manning condensation. Given the dielectric constant of acetonitrile $\varepsilon = 35$, the ^{19}F NMR signal should not be affected below a fraction $f = 0.16$ (for **PG1**) and 0.05 (for **PG2**) of charged or complexed CE moieties. Whereas for

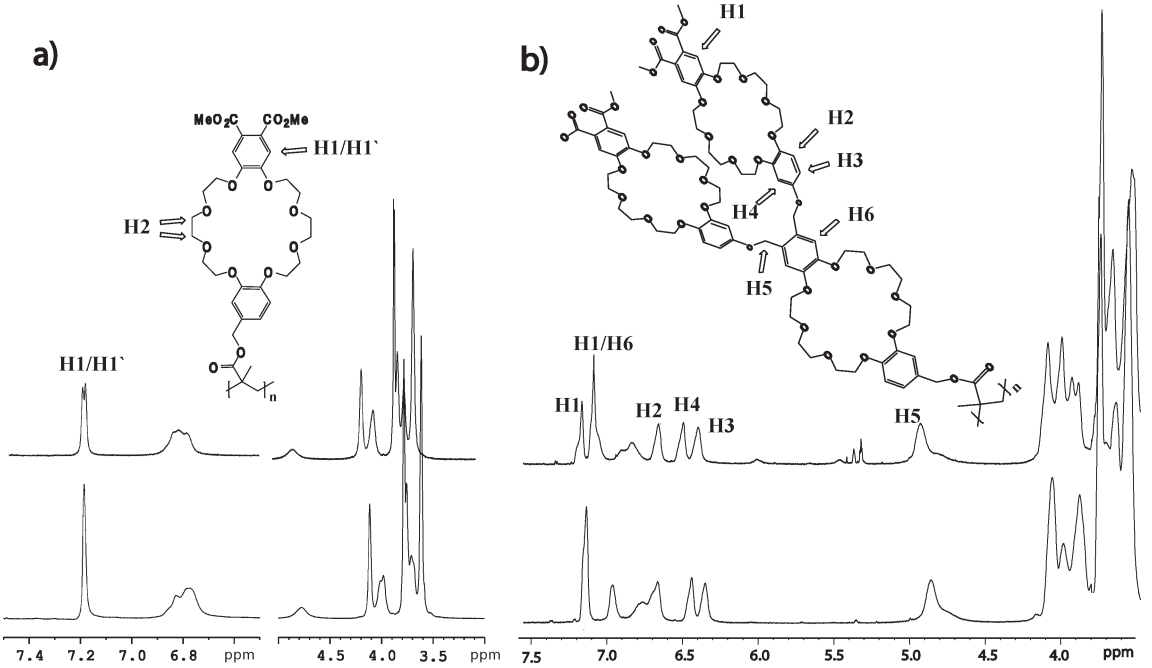

Figure 8. ^{1}H NMR spectra (300 MHz, CD_3CN) of (a) **PG1** (bottom) and **PG1**/KPF_6 (top) ([CE] + [KPF_6] = const. = 7.72×10^{-3} mol/L) and (b) **PG2** (bottom) and **PG2**/KPF_6 (top) ([CE] + [KPF_6] = const. = 1.732×10^{-2} mol/L).

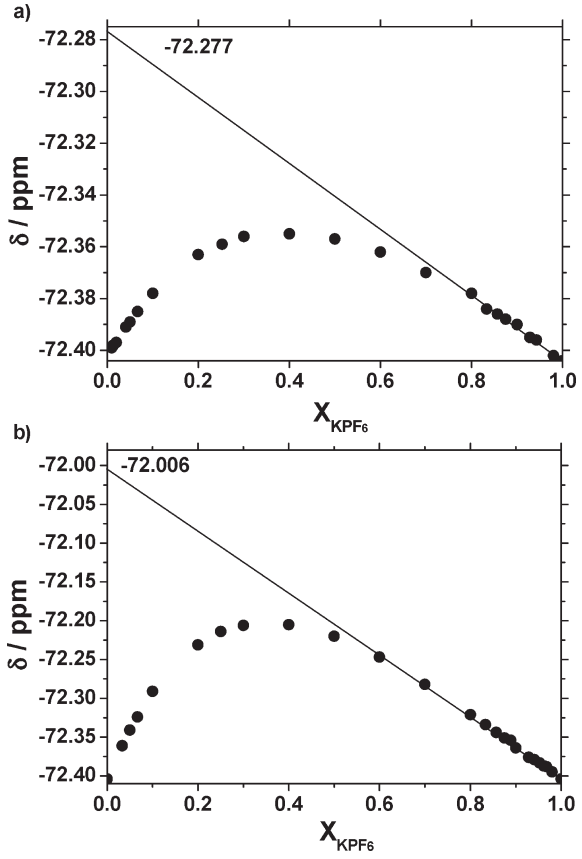

Figure 9. ^{19}F NMR titration curve and linear extrapolation of (a) **PG1**/KPF_6 ([CE] + [KPF_6] = const = 7.72×10^{-3} mol/L) and (b) **PG2**/KPF_6 ([CE] + [KPF_6] = const. = 1.732×10^{-2} mol/L).

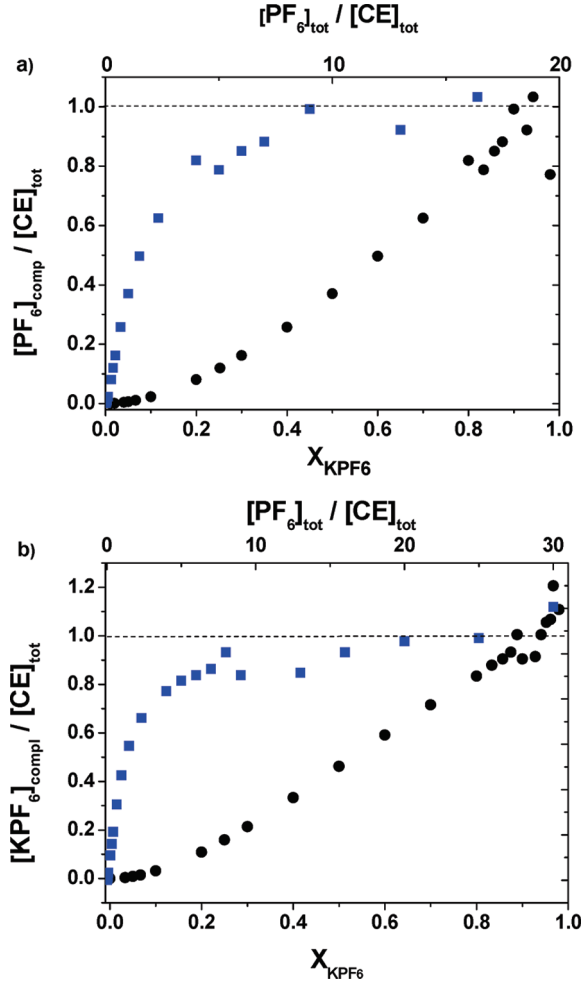

Figure 10. Calculated amount of PF_6^- bound per crown ether at different $[KPF_6]_{total}/[CE]_{total}$ ratios for (a) **PG1**/KPF_6 and (b) **PG2**/KPF_6 with X_{KPF6} = [KPF_6]/([KPF_6] + [CE]) being the molar fraction of KPF_6. Black circles: $[KPF_6]_{compl}/[CE]_{total}$ versus X_{KPF6} (lower scale); Blue squares: $[KPF_6]_{compl}/[CE]_{total}$ versus $[KPF_6]_{total}/[CE]_{total}$ (upper scale).

PG2, this fraction is too low to be clearly resolved, for **PG1**, the chemical shift is clearly observable for $f < 0.15$. Although the validity of the Manning limit for flexible and laterally extended polymers is still controversially discussed, the observed chemical shift of the ^{19}F NMR peaks at K^+ fractions as low as 0.035 is remarkable and qualitatively agrees with very recent results on the effective charge density of poly-2-vinylpyridinium bromides in propanol/pentanone mixtures where Manning's condensation theory could not be experimentally verified.[36,37] To confirm that the observed chemical shift in the ^{19}F NMR spectra is due to counterion binding, we utilized the 2D nuclear Overhauser effect (NOE) NMR technique to monitor the spatial correlation between the PF_6 anions and the protons of the CE.

Whereas the $^1H-^{19}F$ NOE spectra of **MG1** and **9** complexed with KPF_6 do not show any correlation (i.e., a close proximity between the fluorine and the protons of the CE can be excluded), for **PG1** and **PG2** complexed with an excess of KPF_6, the 2D $^1H-^{19}F$ NOE NMR spectrum clearly reveals a correlation between the ^{19}F and both the ethylene glycol protons and the aromatic protons of the CE (Supporting Information), although the latter was weak for the **PG2** sample. Unfortunately, correlations could not be detected for smaller KPF_6 content, most probably because of the limited resolution of the NMR technique.

Upon dissolving the polymers in acetonitrile containing 10^{-2} M KPF_6, that is, an extremely large excess of K^+ ions ($[K^+]/[CE] > 100$, all CEs are assumed to form complexes with K^+ ions. The corresponding light scattering results shown in Figures 11 (**PG1**, Table 1 entry 1) and 12 (**PG2**, Table 1 entry 3) reveal a significant increase in R_g and R_h at constant M_w. Note that the complexation of K^+ does not alter the molar mass detected by light scattering as long as the concentration in the reduced scattering intensity, Kc/R_θ, is calculated by the mass of the uncomplexed polymer, the value for the RI increment, dn/dc, is kept constant at the value measured for the uncomplexed polymer solution, and the RI of the polymer does not change significantly upon K^+-ion complexation. Within experimental error, the molar masses remain constant upon complexation of K^+ ions (Table 2), which confirms the validity of the assumptions made above.

The significant increase in the polymer dimensions upon complexation with K^+ ions could originate from electrostatic expansion of the flexible polymer chains (with increasing charge density) or from the conformational change of the CE side chains, that is, stiffening of the CE ring by K^+ insertion, plus counterion binding and resulting dipole–dipole interactions, or from both. The NMR results presented above suggest the fraction of free K^+ charges along the chain to be very small because PF_6^- counterions immediately compensate the cationic charges by counterion binding, even well below the Manning limit. Because the observed increase in the chain dimensions is small at small K^+ concentrations (as will be shown below), the effect of electrostatic expansions is most likely not significant. Accordingly, steric repulsion between the complexed CE moieties along the chain represents the main driving force for chain expansion.

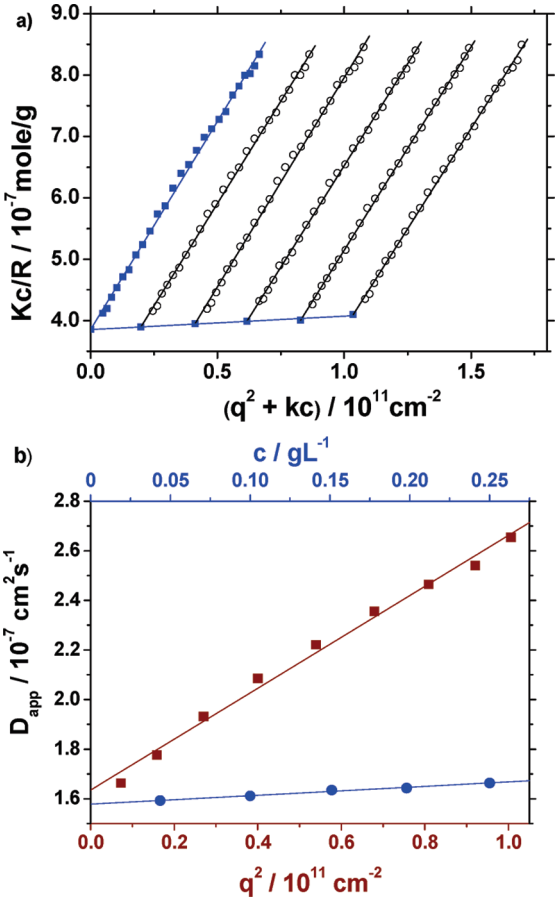

Figure 11. (a) Static Zimm plot and (b) D_{app} versus q^2 (red squares, lower scale, for selected c = 0.151 g/L) and D_{app} (q = 0) versus concentration (blue circles, upper scale) of sample **PG1** in acetonitrile containing 10^{-2} M KPF_6. $M_w = 2.6 \times 10^6$ g/mol, R_g = 72.7 nm, R_h = 36.8 nm.

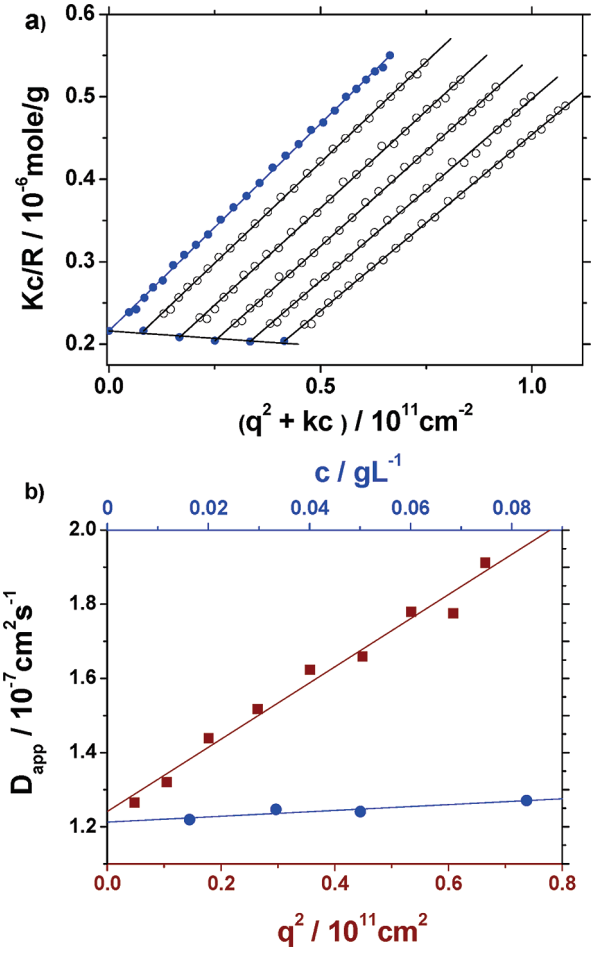

Figure 12. (a) Static Zimm plot and (b) D_{app} versus q^2 (red squares, lower scale, for selected c = 0.0334 g/L) and D_{app} (q = 0) versus concentration (blue circles, upper scale) of sample **PG2 entry 3** in acetonitrile containing 10^{-2} M KPF_6. $M_w = 4.62 \times 10^6$ g/mol, R_g = 84.0 nm, R_h = 48.9 nm.

In view of the small "intrinsic" excluded volume effects, that is, small second virial coefficients, it is thus tempting to analyze the change in the chain dimensions in terms of the Kuhn statistical segment length, l_k, utilizing the Kratky–Porod wormlike chain model[38] with explicit consideration of the main chain polydispersity.[39,40] The weight-average contour length, L_w, derived from M_w has to be related to the square root of the z-average of the mean squared radius of gyration, $< R_g^2 >_z^{0.5}$ and the inverse z-average of the hydrodynamic radius, $< 1/R_h >_z^{-1}$. The results included in Table 2 reveal a significant increase in the Kuhn statistical segment length.

The results for the Kuhn lengths were consistently derived from both R_g and R_h values if the hydrodynamically effective diameter was fixed to d = 3 nm for **PG1** and to d = 6 nm for the **PG2** samples, respectively. These values for d seem to be reasonable given the lateral extension of the CE side chains. The bare Kuhn length of the uncomplexed **PG1 entry 1** polymer, l_k = 8 nm, lies in the expected regime. It is a little bit higher than l_k = 6 nm determined earlier of another first-generation dendronized polymer with a 30% lower molar mass per repeat unit than **PG1**.[4] The formation of the K^+-ion inclusion complex and concomitant counterion binding results in an expanded coil with an increased Kuhn length l_k = 19 nm. A similar increase in l_k is observed for the second generation polymers **PG2 entries 2** and **3**, where the chain stiffness varies from l_k = 19 to 45 nm. Accidentally, the K^+-ion inclusion in **PG1 entry 1** leads to the same Kuhn length as that observed for the uncomplexed **PG2** samples.

To follow the expansion of the polymer chain with increasing cation/CE complexes, the polymer **PG1 entry 1** was dissolved in acetonitrile with 1×10^{-2} M inert PPh_4I at a very low concentration c = 0.05 g/L. Given the small virial coefficient, measurements at this concentration represent the infinite dilution limit within experimental error.

After the addition of KI to this solution (while keeping the polymer concentration constant), the molar mass, M_w, and the dimensions R_g and R_h were monitored as a function of the mole fraction $X_{K+} = [K^+]/([K^+] + [CE])$. The ordinates scatter within experimental error of ~10% because of weighing inaccuracies and possible small filtration losses. (See the Supporting Information.) For better clarity, the form factors $P(q)$, that is, the normalized (by the reduced scattering intensity at q = 0) static scattering curves, are shown in Figure 13. The slope $m = R_g^2/3$ is seen to increase with increasing mole fraction of K^+ ions. In Figure 14, the measured R_g and R_h values (left scale) and the Kuhn statistical segment lengths, l_k (right scale), derived from R_g and R_h by the respective wormlike chain equations, are plotted as function of X_{K+}.

Upon successive complexation of K^+ ions, the dimensions and l_k, accordingly, increase almost linearly for $0 < X_{K+} < 0.8$, followed by a steeper increase toward $X_{K+} = 1$. As discussed above, the small increase in the dimensions for

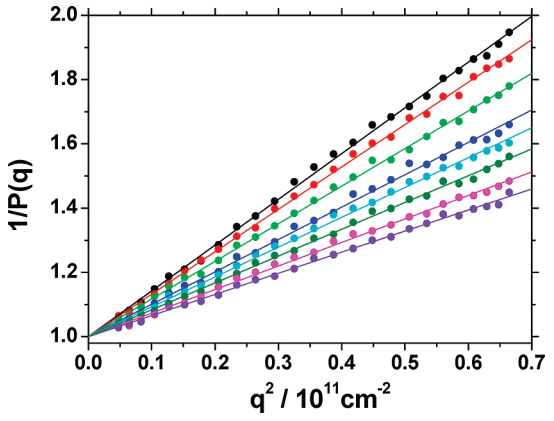

Figure 13. Reduced scattering intensities for **PG1 entry 1** in acetonitrile containing 10^{-2} M PPh_4I and different n_{K+}/n_{crown} ratios (KI concentration from top to bottom 1.97×10^{-3}, 8.40×10^{-4}, 4.36×10^{-4}, 1.44×10^{-4}, 5.50×10^{-5}, 3.75×10^{-5}, 1.95×10^{-5}, and 0 M). The polymer concentration is kept constant at $c = 0.05$ g/L.

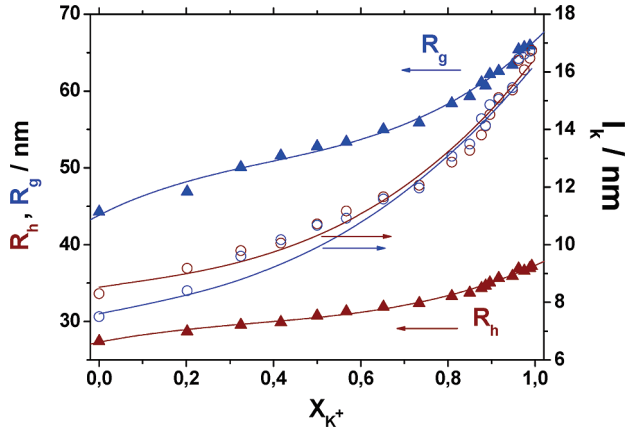

Figure 14. Variation of the dimensions (blue triangle, R_g; red triangle, R_h; left scale) and the respective Kuhn lengths (open blue circle, calculated from R_g; open red circle, calculated from R_h; right scale) with increasing mole fraction of K^+ ions, X_{K+}, measured for **PG1** in 1×10^{-2} M PPh_4I solution in acetonitrile.

small K^+ concentrations renders electrostatic expansion to be negligible. In correspondence with the data in Table 2, the Kuhn length starts at $l_k = 8$ nm for the uncomplexed **PG1** chain and increases to $l_k = 17$ nm, which is slightly below but within experimental error close to the value $l_k = 19$ nm observed for **PG1** in 10^{-2} M KPF_6 solution.

Unfortunately, a more quantitative correlation between the increase in the dimensions in terms of the chain stiffness and the fraction of complexed CE units and bound counterions cannot be made because all efforts to determine the mole fraction of complexed CE units quantitatively by improving the NMR resolution have so far proven to be unsuccessful. The present data reveal a stronger increase in the persistence length above $X_{K+} \approx 0.7$, where according to Figure 8a, the ratio of bound KPF_6 to CE exceeds 0.5. Assuming that this corresponds to a 1:2 ratio of K^+ to CE units, this finding could point toward the formation of 1:2 complexes, as postulated for disk-shaped CEs.[41] However, it is difficult to imagine why the initial formation of 1:2 complexes would lead to only a small increase in chain stiffness and 1:1 complexes would significantly increase chain stiffness.

Alternatively, stiffening of the CE rings upon complexation[42−45] could lead to a larger steric repulsion between the side chains. Therefore, the change of the NMR relaxation time T1 of CE **3** and polymer **PG1** was measured and is summarized in Table 3.

Table 3. T1 Relaxation Times of the Methylene Protons H6 of 3 (c = 9.7 mg/mL, without and with 1 equiv KPF_6) and PG1 (c = 9.7 mg/mL, without and with 3 equiv KPF_6)

	T1 in sec	
proton	without K^+	with K^+
H2 in **PG1** (Figure 8a)	0.71	0.74
corresponding protons in **3**	1.07	0.77

For compound **3**, the T1 becomes shorter from T1 = 1.07 to 0.77 s upon complexation with K^+, as expected. For the uncomplexed polymer T1 = 0.71 s, which means that the degrees of freedom of the CE side chains in the polymer are already reduced, most probably because of the overcrowding effect. Upon complexation, T1 does not change much (T1 = 0.74 s). Therefore, stiffening of the CE side chains upon complexation cannot be the reason for the increasing main chain persistence length.

Therefore, the steric repulsion between the side chains caused by the "loading" of the polymer with KPF_6, which is associated with short-range electrostatic and dipolar interactions between the complexed KPF_6 ion pairs, first weakly and toward high KPF_6 loading strongly increases and causes the chain dimensions and the chain stiffness to increase, accordingly. At full KPF_6 loading, the effect is as large as to triple the molar mass of the side chains. This is evidenced by the similar values of the Kuhn statistical segment length of the fully complexed **PG1** as compared with the noncomplexed **PG2** sample. One has to keep in mind the fact that the KPF_6 loading increases the polarity in the inner part of the dendron side chains, which may attract additional solvent molecules.

Conclusions

The conformation of dendronized polymers with CE side chains can be manipulated by complexation with K^+ ions. The chain dimensions were observed to increase by up to 80% depending on the main chain length and on the side chain generation. It is concluded that polymers with comparatively small CE side chains constitute an attractive alternative to sometimes painful synthetic efforts toward higher-generation dendronized polymers to achieve similar chain stiffness by simple complexation of metal ions. The ultimate goal of the work to obtain even larger stiffening effects by electrostatic repulsion of the complexed CE side chains could not be realized because of the remarkable absence of any significant electrostatic stiffening at small K^+ loading. This is in qualitative agreement with recent results[36,37] on quaternized polyvinylpyridines in propanol, which reveal a much smaller effective charge density of polyelectrolytes in organic solvents of low dielectric constant (smaller than water) as compared with Manning condensation and as typically observed in aqueous solution.

Experimental Section

Materials. Triethylene glycol monotosylate (TEG-Ts) was synthesized according to literature procedure.[46] Compounds **1** and **2** were synthesized as described by Koch[47] and Stoddart,[48] respectively. Azobis(*iso*-butyronitrile) (AIBN) was recrystallized twice from methanol. Tetrahydrofuran (THF) was refluxed over sodium/benzophenone and DCM distilled from CaH_2 for drying. Other reagents and solvents were purchased at reagent grade and used without further purification. Macherey-Nagel precoated TLC plates (silica gel 60 G/UV_{254}, 0.25 mm) were used for thin-layer chromatography (TLC) analysis. Silica

gel 60 M (Macherey-Nagel, 0.04 to 0.063 mm, 230−400 mesh) was used as the stationary phase for column chromatography.

Measurements. ^{1}H and ^{13}C NMR spectra were recorded on Bruker Avance 200, 300, 500, or 700 spectrometers. The NMR titration spectra were recorded on either a Bruker Avance 500 or 700 spectrometer. For the titrations of **MG1**, **9**, **PG1** and **PG2**, a stock solution of the respective compound and a stock solution of KPF_6 in CD_3CN were prepared. The appropriate volumes of the solutions were mixed in such a way that the sum of the concentrations of CEs remained constant ([CE(MG1)] + [KPF_6] = 7.55×10^{-3} mol/L; [CE(PG1)] + [KPF_6] = 7.72×10^{-3} mol/L; [CE(PG2)] + [KPF_6] = 1.73×10^{-2} mol/L). For the titration of **9**, the concentration of the CE was kept constant ([CE] = 1.9×10^{-3} mol/L) at all measurements.

Chemical shifts are reported as δ values (ppm) relative to internal Me_4Si standard. High-resolution MALDI analyses were performed by the MS service of the Laboratorium für Organische Chemie, ETH Zürich, on IonSpec Ultra instruments. T1 measurements were recorded on a Bruker Avance 500 and T1 was calculated by $I[t] = I[0] + P^* \exp(-t/T1)$ over 16 data points. Elemental analyses were performed by the Mikrolabor of the Laboratorium für Organische Chemie, ETH Zürich. Gel permeation chromatography (GPC) measurements were carried out by using a PL-GPC 220 instrument with a 2× PL-Gel Mix-B LS column set (2 × 30 cm) equipped with refractive index (RI) detector, and LiBr (1 g/L) in DMF (45 °C) or $CHCl_3$ (35 °C) as the eluent. Standard calibration was performed with polymethylmethacrylate standards in the range of M_p = 7800 to 1 520 000 (Polymer Laboratories, U.K.). The glass transient temperature (T_g) was taken in the second heating run. Samples for elemental analysis and all monomers for polymerization were purified additionally to column chromatography with a Japan Analytical Industry LC-9101 recycling HPLC (2 columns, 2H, 2.5H) with chloroform as the eluent.

Light Scattering. Static and dynamic light scattering measurements were performed either with an ALV-SP86 goniometer, an Uniphase HeNe laser (25 mW output power at 632.8 nm wavelength), an ALV/High QE APD avalanche diode fiberoptic detection system and an ALV-3000 correlator or with an ALV-SP125 goniometer, a Spectra Physics Ar-ion laser (operating with 500 mW output power at 514.5 nm wavelength) and an ALV-5000 correlator. In the latter setup, the scattering intensity was split onto two photomultipliers, the signals of which were cross-correlated to eliminate systematic electronic correlations.

The static scattering intensities were analyzed according to standard procedures in terms of Zimm plots yielding the weight-average molar mass, M_w, the mean square radius of gyration, $R_g^2 = < R_g^2 >_z$, and the second virial coefficient, A_2.

The correlation functions taken from the solutions with added PPh_4Br salt showed a very fast decay with a small amplitude, followed by a broad but monomodal decay. Control measurements of pure salt solutions could identify the fast mode to originate from the diffusion of the bulky salt yielding $D_{PPh4Br} = 1.08 \times 10^{-5}$ cm^2/sec. Therefore, the correlation functions taken from the polymer solutions were fitted by a sum of three exponentials. The decay of the first one was fixed to the measured salt diffusion, and from the other two relaxation processes, the first cumulant Γ was calculated. For the solutions with added KPF_6 salt, only, no fast mode could be detected; accordingly, a sum of two exponentials was utilized to fit the data. The z-average diffusion coefficient D_z was obtained by extrapolation of Γ/q^2 to $q = 0$ and to infinite dilution. The inverse z-average hydrodynamic radius $R_h = < 1/R_h >_z^{-1}$ was evaluated by formal application of Stokes law.

The dilute polymer solutions in acetonitrile plus the respective salts, as indicated in the main text (typically four to five concentrations $0.01 \le c \le 0.6$ mg/mL), were measured from 30 to 150° in steps of 5 (SLS) or 10° (DLS). Prior to measurement, the solutions were filtered through 0.45 μm pore size filters (Millipore GHP).

The errors for the determination of M_w were smaller than ±5%, of R_g and R_h smaller than ±3%.

The RI increments were measured by a home-built Michelson interferometer, as described elsewhere,[49] and determined to $dn/dc = 0.1705$ for **PG1** (entry 1 in Table 1) and $dn/dc = 0.1878$ cm^3/g for **PG2** (entry 3 in Table 1) in acetonitrile with 10^{-2} M PPh_4Br.

Syntheses. *Dimethyl 16-Formyl-6,7,9,10,12,13,20,21,23,24,26,27-dodecahydrodibenzo[b,n][1,4,7,10,13,16,19,22]octaoxacyclotetracosine-2,3-dicarboxylate* (***3***). A solution of dimethyl 4,5-dihydroxyphthalate (8.67 g, 38.33 mmol), **2** (27.25 g, 38.33 mmol) and KPF_6 (7.06 g, 38.33 mmol) in acetonitrile (1 L) was added dropwise over a period of 12 h to a suspension of K_2CO_3 (52.98 g, 383.32 mmol) in CH_3CN at 60 °C. After complete addition, the mixture was stirred for an additional 12 h at this temperature. After evaporation of the solvent at reduced pressure, the residue was dissolved in $CHCl_3$ (600 mL) and water (500 mL). After separation of the organic phase, the water phase was extracted with 300 mL of $CHCl_3$. The combined organic phases were washed with brine (300 mL) and dried with $MgSO_4$. After evaporation of the solvent in vacuo, the resulting viscous oil was purified by column chromatography ($CHCl_3$/MeOH 95:5 v/v) to afford the product as a white solid (17.20 g, 76%). R_f = 0.22 ($CHCl_3$/MeOH 95:5 v/v). mp 102−106 °C. ^{1}H NMR (300 MHz, DMSO-d_6, δ): 3.67 (s, 8 H, OCH_2CH_2O), 3.70−3.85 (m, 8 H, $ArOCH_2CH_2$ and 6 H, CO_2CH_3), 4.10−4.25 (m, 8 H, $ArOCH_2$), 7.15 (d, J = 8 Hz, 2 H, Ar−H), 7.23 (s, 2H, Ar−H), 7.38 (d, J = 2 Hz, 1 H, Ar−H), 7.52 (dd, J = 2 Hz, J = 8 Hz, 1 H, Ar−H), 9.81 (s, 1 H, CHO); ^{13}C NMR (75 MHz, $CDCl_3$, δ): 190.91, 167.82, 167.77, 154.24, 150.40, 150.37, 149.12, 130.25, 126.92, 125.39, 113.21, 113.17, 111.92, 111.05, 71.48, 71.44, 69.69, 69.62, 69.54, 69.39, 52.63. MS (ESI) (m/z): calcd for $C_{29}H_{36}O_{13}Na$, 615.21; found 615.3 $[M + Na]^+$ (100%), 561.3 $[M-OMe]^+$ (25%). Anal. Calcd for $C_{29}H_{36}O_{13}$: C, 58.78; H, 6.12; O, 35.10. Found: C, 58.50; H, 5.93; O, 35.22.

Dimethyl 16-(Hydroxymethyl)-6,7,9,10,12,13,20,21,23,24,26,27-dodecahydrodibenzo[b,n][1,4,7,10,13,16,19,22]octaoxacyclotetracosine-2,3-dicarboxylate (***4***). To a solution of compound **3** (2 g, 3.38 mmol) in THF (70 mL) at room temperature, MeOH (15 mL) was added. Every 15 min, $NaBH_4$ (40 mg, 1.06 mmol) was added to the solution until TLC did not show any starting material anymore (after four to five portions). The reaction was neutralized with 0.1 M HCl and diluted with $CHCl_3$ (300 mL) and brine (300 mL). The phases were separated, and the organic layer was washed with saturated $NaHCO_3$ solution and dried over $MgSO_4$. The solvent was evaporated under reduced pressure to give a colorless solid material that was used without further purification in the next reaction. Yield: 1.91 g (95%). R_f = 0.35 ($CHCl_3$/MeOH 9:1 v/v). mp 94.8−96.2 °C. ^{1}H NMR (300 MHz, $CDCl_3$, δ): 1.91 (br, 1 H, OH), 3.84 (s, 8 H, OCH_2CH_2O), 3.89 (s, 6 H, OCH_3), 3.94 (m, 8 H, OCH_2CH_2O), 4.15 (m, 4 H, $ArOCH_2CH_2O$), 4.21 (m, 4 H, $ArOCH_2CH_2O$), 6.8−6.9 (m, 3 H, Ar−H), 7.17 (s, 2 H, Ar−H). ^{13}C NMR (125 MHz, $CDCl_3$, δ): 168.28, 168.20, 150.83, 150.79, 149.31, 148.66, 134.69, 125.72, 125.59, 120.22, 114.10, 113.52, 113.50, 113.17, 71.89, 71.86, 71.69, 70.31, 70.27, 69.92, 69.90, 69.86, 69.68, 67.48, 65.49, 52.99. MS (HiRes MALDI, 3-HPA) (m/z): calcd for monoisotopic peak $^{12}C_{29}{}^1H_{38}{}^{16}O_{13}{}^{23}Na$, 617.2210; found, 617.2215. Anal. Calcd for $C_{29}H_{38}O_{13}$: C, 58.58; H, 6.44; O, 34.98. Found: C, 58.59; H, 6.49; O, 35.07.

Dimethyl 16-(Methacryloyloxymethyl)-6,7,9,10,12,13,20,21,23,24,26,27-dodecahydro dibenzo[b,n][1,4,7,10,13,16,19,22]octaoxacyclotetracosine-2,3-dicarboxylate (***MG1***). Compound **8** (740 mg, 1.24 mmol) was dissolved in THF (50 mL) at room temperature. TEA (251.9 mg, 2.5 mmol) and MAC (286.2 mg, 2.74 mmol) were added subsequently. After 30 min, no starting material was visible by TLC anymore. The reaction mixture was diluted with DCM (100 mL) and washed with 1 M $NaHSO_4$ and water. The organic phase was dried over $MgSO_4$, and the solvent was evaporated under reduced pressure at 30 °C. The residue was purified by column chromatography on silica gel (ethyl acetate). Yield: 620 mg (75%). R_f = 0.38 ($CHCl_3$/MeOH

95:5 v/v). mp 79−84 °C. ^{1}H NMR (300 MHz, $CDCl_3$, δ): 1.95 (s, 3 H, CH_3), 3.75−3.98 (m, 16 H, OCH_2CH_2O), 3.87 (s, 6 H, CO_2CH_3), 4.10−4.25 (m, 8 H, OCH_2CH_2O), 5.10 (s, 2 H, Bz-H), 5.67 (s, 1 H, vinyl-H), 6.12 (s, 1 H, vinyl-H), 6.80−6.95 (m, 3 H, Ar−H), 7.17 (s, 2 H, Ar−H). ^{13}C NMR (75 MHz, $CDCl_3$, δ): 167.66, 167.13, 150.35, 148.79, 148.72, 136.18, 129.07, 125.58, 125.22, 121.43, 114.10, 113.51, 113.12, 71.36, 71.19, 69.64, 69.44, 69.36, 66.97, 66.22, 52.43, 18.23. MS (HiResMALDI, 3-HPA) (m/z): calcd for monoisotopic peak $^{12}C_{33}{}^{1}H_{42}{}^{16}O_{14}{}^{23}Na$, 685.2472; found, 685.2478. Anal. Calcd: C, 59.81; H, 6.39; O, 33.80. Found C, 59.62; H, 6.41; O, 33.76.

Dimethyl 16-(1,3-Dioxan-2-yl)-6,7,9,10,12,13,20,21,23,24,26,27-dodecahydro-dibenzo[b,n][1,4,7,10,13,16,19,22]octaoxacyclotetracosine-2,3-dicarbo-xylate (***5***). The compound **3** (15.00 g, 25.3 mmol) and 4-methylbenzenesulfonic acid monohydrate (963 mg, 5 mmol) were dissolved in benzene (500 mL) and heated to reflux. A dean stark was used for water separation. 1,3-Dihydroxypropane (9.63 g, 126.6 mmol) was added in three portions every 2 h. The solution was refluxed for 16 h. After cooling to room temp, the reaction was quenched with pyridine (5 mL) and washed with saturated $NaHCO_3$ solution (250 mL) and brine (250 mL) successively. The organic phase was dried with $MgSO_4$,and the solvent was evaporated under reduced pressure. The crude product was recrystallized from methanol to give a colorless solid (15.49 g, 94%) material. R_f = 0.55 ($CHCl_3$/MeOH 9:1 v/v). mp 122−124 °C, ^{1}H NMR (300 MHz, $CDCl_3$, δ): 1.45 (m, 1 H, acetal-H), 2.25 (m, 1 H, acetal-H), 3.84 (s, 8 H, OCH_2CH_2O), 3.91 (s, 6 H, OCH_3), 3.94 (m, 8 H, OCH_2CH_2O), 3.99 (d, J = 2.11 Hz, 1 H, acetal-H), 4.03 (d, J = 2.27 Hz, 1 H, acetal-H), 4.16 (d, J = 4.46 Hz, 1 H, acetal-H), 4.22 (m, 8 H, OCH_2CH_2O), 4.28 (d, J = 4.92 Hz, 1 H, acetal-H), 5.44 (s, 1 H, Bz-H), 6.86 (d, J = 8.21 Hz, 1 H, Ar−H), 7.02 (dd, J = 1.63 Hz, 8.26 Hz, 1 H, Ar−H), 7.05 (d, J = 1.59 Hz, 1 H, Ar−H), 7.19 (s, 2 H, Ar−H). ^{13}C NMR (75 MHz, $CDCl_3$, δ): 167.79, 150.50, 149.13, 148.74, 132.18, 125.32, 119.08, 113.46, 113.27, 111.45, 101.43, 71.45, 71.28, 71.25, 69.87, 69.62, 69.61, 69.53, 69.37, 67.34, 52.53, 25.72. Anal. Calcd: C, 59.07; H, 6.51; O, 34.42. Found: C, 59.21; H, 6.53; O, 34.39. MS (MALDI-TOF, DCTB + Na-TFA mix 1:10) (m/z): calcd for $^{12}C_{32}{}^{1}H_{42}{}^{16}O_{14}{}^{23}Na$, 673.25; found, 673.23.

(*16-(1,3-Dioxan-2-yl)-6,7,9,10,12,13,20,21,23,24,26,27-dodecahydrodibenzo[b,n][1,4,7,10,13,16,19,22]octaoxacyclotetracosine-2,3-diyl)dimethanol* (***6***). DIBAL-H (67.21 g, 20 wt % in toluene, 94.5 mmol) was added dropwise over a period of 30 min to a solution of CE **4** (12.30 g, 18.90 mmol) in 400 mL of dry THF under a nitrogen atmosphere at room temperature. After 2 h, the reaction was quenched by the careful addition of brine (300 mL) and water (1 L). The organic phase was diluted with $CHCl_3$ (300 mL). After phase separation, the water phase was extracted five times with $CHCl_3$. The combined organic phases were dried over $MgSO_4$, and the solvent was evaporated under reduced pressure. A colorless solid material (10.57 g, 94%) was obtained, which was used in the next step without further purification. R_f = 0.36 ($CHCl_3$/MeOH 8:2 v/v). mp 108−116 °C. ^{1}H NMR (300 MHz, $CDCl_3$, δ): 1.46 (m, 1 H, acetal-H), 2.23 (m, 1 H, acetal-H), 3.07 (s, 2 H, OH), 3.82 (s, 8 H, OCH_2CH_2O), 3.91 (m, 8 H, OCH_2CH_2O), 3.98 (d, J = 2.08 Hz, 1 H, acetal-H), 4.02 (d, J = 2.27 Hz, 1 H, acetal-H), 4.16 (m, 8 H, OCH_2CH_2O), 4.24 (d, J = 4.93 Hz, 1 H, acetal-H), 4.28 (d, J = 4.89 Hz, 1 H, acetal-H), 4.60 (s, 4 H, Bz-H), 5.44 (s, 1 H, acetal-H), 6.84 (d, J = 8.25 Hz, 1 H, Ar−H), 6.87 (s, 2 H, Ar−H), 7.00 (dd, J = 1.75 Hz, 8.21 Hz, 1 H, Ar−H), 7.03 (d, J = 1.65 Hz). ^{13}C NMR (50 MHz, $CDCl_3$, δ): 149.11, 148.70, 148.21, 132.76, 132.15, 119.16, 115.81, 113.53, 111.54, 101.46, 71.19, 69.85, 69.76, 69.49, 69.38, 69.27, 67.37, 67.09, 63.53, 25.72. MS (HiRes MALDI, 3-HPA) (m/z): calcd for monoisotopic peak $^{12}C_{30}{}^{1}H_{42}{}^{16}O_{12}{}^{23}Na$, 617.2574; found, 617.2580 $[M + Na]^+$. Anal. Calcd for $C_{30}H_{42}O_{12}$: C, 60.59; H, 7.12; O, 32.29. Found: C, 60.30; H, 7.07; O 32.37.

16,17-Bis(chloromethyl)-6,7,9,10,12,13,20,21,23,24,26,27-dodecahydrodibenzo[b,n][1,4,7,10,13,16,19,22]octaoxacyclotetracosine-2-carbaldehyde (***7***). A solution of **5** (3.97 g, 6.7 mmol in 60 mL of DCM) was added dropwise to a solution of $SOCl_2$ (7.94 g) in DCM (60 mL) and 2 drops of DMF at −10 °C. The reaction mixture was allowed to warm up to 0 °C. After 2 h, the green solution was carefully poured into a saturated $NaHCO_3$ solution. The phases were separated, the water phase was extracted with DCM (200 mL), and the combined organic phase was washed with water. The organic phase was dried with $MgSO_4$, and the solvent was evaporated under reduced pressure. The residue was purified by column chromatography on silica gel ($CHCl_3$/MeOH 9:1 v/v) to give 3.46 g (82%) of a colorless solid. R_f = 0.51 ($CHCl_3$/MeOH 9:1 v/v). ^{1}H NMR (300 MHz, $CDCl_3$, δ): 3.84 (m, 8 H, OCH_2CH_2O), 3.94 (m, 8 H, OCH_2CH_2O), 4.20 (m, 8 H, OCH_2CH_2O), 4.68 (s, 4 H, $ArCH_2$-Cl), 6.88 (s, 2 H, Ar−H), 6.95 (d, J = 8.15 Hz, 1 H, Ar−H), 7.29 (d, J = 1.30 Hz, 1 H, Ar−H), 7.43 (dd, J = 8.20 Hz, 1.33 Hz, 1 H, Ar−H), 9.83 (s, 1 H, aldehyde-H). ^{13}C NMR (75 MHz, $CDCl_3$, δ): 190.83, 154.30, 149.19, 149.16, 130.22, 129.15, 129.11, 126.79, 115.85, 115.83, 111.93, 111.10, 71.54, 71.43, 71.37, 69.75, 69.70, 69.63, 69.54, 69.45, 69.39, 43.34. MS (HiRes MALDI, 3-HPA) (m/z): calcd for monoisotopic peak $^{12}C_{27}{}^{1}H_{34}{}^{35}Cl_2{}^{16}O_9{}^{23}Na$, 595.1472; found, 595.1463 $[M + Na]^+$; calcd for monoisotopic peak $^{12}C_{27}{}^{1}H_{34}{}^{35}Cl_2{}^{16}O_9{}^{39}K$, 611.1217; found, 611.1205 $[M + K]^+$.

Dimethyl 16-Hydroxy-6,7,9,10,12,13,20,21,23,24,26,27-dodecahydrodibenzo[b,n][1,4,7,10,13,16,19,22]octaoxacyclotetracosine-2,3-dicarboxylate (***8***). To a suspension of **3** (2.22 g, 3.75 mmol) in MeOH (40 mL) H_2O_2 (2 g, 30 wt % in H_2O, 17.65 mmol) and concentrated H_2SO_4 (0.5 mL) were subsequently added. While being heated to 60 °C, the compound was dissolved, and the solution was stirred for 2 days at this temperature. After cooling down to room temperature, the reaction mixture was neutralized with saturated $NaHCO_3$ solution. The mixture was extracted with DCM (3 × 100 mL), and the combined organic phases were washed with brine. The solvent was evaporated under reduced pressure, and the residue was purified by column chromatography on silica gel ($CHCl_3$/MeOH 94:6 v/v). Yield: 1.28 g (59%) of dark red oil. R_f = 0.23 ($CHCl_3$/MeOH 95:5, v/v). ^{1}H NMR (300 MHz, $CDCl_3$, δ): 3.79 (broad s, 8 H, OCH_2CH_2O), 3.82−3.94 (m, 8 H, OCH_2CH_2O), 3.87 (s, 6 H, OCH_3), 4.06 (m, 4 H, OCH_2CH_2O), 4.17 (m, 4 H, OCH_2CH_2O), 5.40 (broad s, 1 H, ArOH), 6.26 (dd, J = 8.56 Hz, 2.70 Hz, 1 H, Ar−H), 6.38 (d, J = 2.71 Hz, 1 H, Ar−H), 6.68 (d, J = 8.58 Hz, 1 H, Ar−H), 7.15 (s, 2 H, Ar−H). ^{13}C NMR (75 MHz, $CDCl_3$, δ): 167.97, 167.91, 151.318, 150.40, 149.91, 142.19, 125.18, 125.23, 116.22, 113.21, 113.15, 106.79, 102.36, 71.38, 71.14, 70.98, 70.32, 70.14, 69.77, 69.49, 69.45, 69.39, 68.84, 52.64. Anal. Calcd for $C_{28}H_{36}O_{13}$: C, 57.93; H, 6.25; O, 35.82. Found: C, 56.97; H 6.40; O, 35.48. MS (HiRes MALDI, 3-HPA) (m/z): calcd for monoisotopic peak $^{12}C_{28}{}^{1}H_{36}{}^{16}O_{13}{}^{23}Na$, 603.2048; found, 603.2057.

Tetramethyl 16,16′-(16-Formyl-6,7,9,10,12,13,20,21,23,24,26,27-dodecahydrodibenzo[b,n][1,4,7,10,13,16,19,22]octaoxacyclotetracosine-2,3-diyl)bis(methylene)bis(oxy) bis(6,7,9,10,12,13,20,21,23,24,26,27-dodecahydrodibenzo[b,n][1,4,7,10,13,16,19,22]octaoxacyclotetracosine-2,3-dicarboxylate) (***9***). A solution of compound **6** (3.40 g, 5.93 mmol) and compound **7** (8.6 g, 14.81 mmol) in DMF (100 mL) was added to a suspension of $CsCO_3$ (19.31 g, 59.25 mmol) and KI (4.92 g, 29.63 mmol) under a nitrogen atmosphere at room temperature. The reaction mixture was then heated to 60 °C for 15 h. After cooling to room temperature, the reaction mixture was diluted with $CHCl_3$ (300 mL) and 1 M $NaHSO_4$ (300 mL). The phases were separated, and the organic phase was washed with brine and water subsequently. After the organic phase was dried with $MgSO_4$, the solvent was evaporated under reduced pressure. The residue was purified by column chromatography on silica gel (EE/MeOH 9:1 → DCM/MeOH 9:1 v/v) to give a colorless amorphous material. Yield: 6.30 g (64%). R_f = 0.32 ($CHCl_3$/MeOH 9:1). ^{1}H NMR (300 MHz, $CDCl_3$, δ): 3.80−3.87 (m, 24 H, OCH_2CH_2O), 3.88−4.01

(m, 36 H, OCH_2CH_2O, CO_2CH_3), 4.06−4.15 (m, 8 H, OCH_2CH_2O), 4.15−4.28 (m, 16 H, OCH_2CH_2O), 4.98 (s, 4 H, Bz-H), 6.44 (dd, $J = 8.50$ Hz, 2.67 Hz, 2 H, Ar−H), 6.54 (d, $J =$ 2.67 Hz, 2 H, Ar−H), 6.80 (d, $J = 8.75$, 2 H, Ar−H), 6.96 (d, $J =$ 8.25, 1 H, Ar−H), 7.01 (s, 2 H, Ar−H), 7.19 (s, 4 H, Ar−H), 7.40 (d, $J = 1.67$ Hz, 1 H, Ar−H), 7.44 (dd, $J = 8.16$ Hz, 1.70 Hz, 1 H, Ar−H), 9.85 (s, 1 H, CHO). ^{13}C NMR (75 MHz, $CDCl_3$, δ): 190.85, 167.79, 167.78, 154.32, 153.81, 150.49, 150.47, 150.07, 149.20, 148.63, 148.62, 143.40, 130.21, 128.30, 126.79, 125.37, 125.34, 113.32, 113.27, 111.95, 111.14, 105.26, 102.98, 71.52, 71.42, 71.31, 71.26, 71.11, 70.35, 70.11, 69.85, 69.81, 69.70, 69.59, 69.56, 69.53, 69.44, 69.40, 69.19, 68.16, 52.55. Anal. Calcd for $C_{83}H_{104}O_{35}$: C, 59.99; H, 6.31; O, 33.70. Found: C, 59.81; H, 6.56; O, 33.73. MS (HiRes MALDI, 3-HPA) (m/z): calcd for monoisotopic peak $^{12}C_{83}{}^{1}H_{104}{}^{16}O_{35}{}^{23}Na$, 1683.626; found, 1683.628 $[M + Na]^+$; calcd for monoisotopic peak $^{12}C_{83}{}^{1}H_{104}{}^{16}O_{35}{}^{39}K$, 1699.600; found, 1699.605 $[M + K]^+$.

Tetramethyl 16,16′-(16-(Hydroxymethyl)-6,7,9,10,12,13,20,21,23, 24,26,27-dodeca-hydrodibenzo[b,n][1,4,7,10,13,16,19,22]octaoxa-cyclotetracosine-2,3-diyl)bis-(methylene)bis(oxy)bis(6,7,9,10,12,13, 20,21,23,24,26,27-dodecahydrodibenzo[b,n][1,4,7,10,13,16,19,22]-octaoxacyclotetracosine-2,3-dicarboxylate) (***10***). Compound **9** (520 mg, 313 μmol) was dissolved in THF (75 mL) before MeOH (50 mL) was added. Then, $NaBH_4$ (6 mg, 157 μmol) was added in one portion. The reaction was monitored by TLC until no starting material was observed any more (20 min.). The reaction was quenched with distilled H_2O (20 mL) and three drops of HCl (25%). After 15 min, $CHCl_3$ (100 mL) was added, and the phases were separated. The water phase was washed with $CHCl_3$, and the combined organic phases were washed with saturated $NaHCO_3$ solution. The organic phase was dried over $MgSO_4$, and the solvent was evaporated under reduced pressure. The product was used in the next step without further purification. Yield: 510 mg (98%) of a colorless amorphous material. $R_f = 0.56$ ($CHCl_3$/MeOH 8:2 v/v). ^{1}H NMR (300 MHz, $CDCl_3$, δ): 3.82 (s, 24 H, OCH_2CH_2O), 3.84−3.98 (m, 24 H, OCH_2CH_2O and 12 H, OCH_3), 4.04−4.25 (m, 24 H, OCH_2CH_2O), 4.57 (s, 2 H, Bz-H), 4.96 (s, 4 H, Bz-H), 6.42 (dd, $J = 8.76$ Hz, 2.51 Hz, 2 H, Ar−H), 6.52 (d, $J = 2.53$ Hz, 2 H, Ar−H), 6.77 (d, $J = 8.74$ Hz, 2 H, Ar−H), 6.82−6.92 (m, 2 H, Ar−H), 6.70 (s, 2 H, Bz-H), 7.17 (s, 4 H, Bz-H). ^{13}C NMR (50 MHz, $CDCl_3$, δ): 167.79, 153.81, 150.48, 150.07, 148.68, 143.40, 128.31, 125.34, 125.34, 119.86, 115.67, 115.30, 113.29, 105.31, 103.00, 71.42, 71.26, 71.11, 70.35, 70.11, 61.91, 69.82, 69.19, 68.19, 65.03, 52.56. MS (HiRes MALDI, 3-HPA) (m/z): calcd for monoisotopic peak $^{12}C_{83}{}^{1}H_{106}{}^{16}O_{35}{}^{23}Na$, 1685.641; found, 1685.637.

Tetramethyl 16,16′-(16-(Methacryloyloxymethyl)-6,7,9,10,12, 13,20,21,23,24,26,27-dodecahydrodibenzo[b,n][1,4,7,10,13,16,19,22]-octaoxacyclotetracosine-2,3-diyl)bis(methylene)bis(oxy)bis(6,7,9, 10,12,13,20,21,23,24,26,27-dodecahydrodibenzo[b,n] [1,4,7,10, 13,16,19,22]octaoxacyclotetracosine-2,3-dicarboxylate) (***MG2***). Compound **10** (520 mg, 313 μmol) was dissolved in THF (35 mL) and cooled to 0 °C. Subsequently, LiBr (54.3 mg, 625 μmol), TEA (150 mg, 1.48 mmol), and MAC (180 mg, 1.72 mmol) were added. After 4 h, an additional 0.5 mL of MAC was added, and the reaction was allowed to warm to room temperature overnight. The solution was diluted with DCM (100 mL) and washed with 1 M $NaHSO_4$ (50 mL) and brine subsequently. The solution was dried over $MgSO_4$, and the solvent was evaporated under reduced pressure. The residue was purified by column chromatography on silica gel (EE/MeOH 9:1 v/v). Yield: 450 mg (83%) of a colorless amorphous material. $R_f = 0.72$ ($CHCl_3$/MeOH 9:1 v/v). ^{1}H NMR (300 MHz, $CDCl_3$, δ): 1.94 (s, 3 H, allyl-CH_3), 3.75−3.97 (m, 60 H, OCH_2CH_2O and OCH_3), 4.03−4.12 (m, 8 H, OCH_2CH_2O, 4.12−4.25 (m, 24 H, OCH_2CH_2O), 4.95 (s, 4 H, Bz-H), 5.09 (s, 2 H, Bz-H), 5.56 (s, 1 H, vinyl-H), 6.12 (s, 1 H, vinyl-H), 6.42 (dd, $J = 8.73$ Hz, 2.64 Hz, 2 H, Ar−H), 6.51 (d, $J = 2.64$ Hz, 2 H, Ar−H), 6.77 (d, $J = 8.75$ Hz, 2 H, Ar−H), 6.80−6.95 (m, 3 H, Ar−H), 6.99 (s, 2 H, Ar−H), 7.17 (s, 4 H, Ar−H). ^{13}C NMR (50 MHz, $CDCl_3$, δ): 167.77, 167.20, 153.81, 150.49, 150.47, 150.05, 148.94, 148.86, 148.66, 143.38, 136.28, 129.20, 128.32, 125.71, 125.36, 125.33, 121.57, 115.66, 115.29, 114.32, 113.73, 113.32, 113.27, 105.29, 102.98, 71.39, 71.23, 71.08, 70.32, 70.09, 69.83, 69.54, 69.46, 69.15, 68.18, 66.33, 52.55, 18.35. MS (HiRes MALDI, 3-HPA) (m/z): calcd for monoisotopic peak $^{12}C_{87}{}^{1}H_{110}{}^{16}O_{36}{}^{23}Na$, 1753.667; found, 1753.663 $[M + Na]^+$. Anal. Calcd for $C_{87}H_{110}O_{36}$: C, 60.34; H, 6.40; O, 33.26. Found: C, 60.07; H, 6.65; O, 33.51.

Poly(dimethyl 16-(Methacryloyloxymethyl)-6,7,9,10,12,13,20, 21,23,24,26,27-dodeca-hydrodibenzo[b,n][1,4,7,10,13,16,19,22]octa-oxacyclotetracosine-2,3-dicarboxylate) (***PG1***). Monomer **9** (200 mg) was dissolved in 0.2 mL of DMF at 30 °C, and 0.4 mg of freshly recrystallized AIBN in 20 μL of DMF was added. The solution was then placed in a preheated oil bath at 60 °C after careful degassing by three freeze−pump−thaw circles. After 16 h, the solution was cooled to room temperature and filtered over a short silica gel column with $CHCl_3$ as eluent. Yield: 194 mg (97%) of a colorless powder. ^{1}H NMR (300 MHz, $CDCl_3$, δ): 0.7 (br, 2 H, CH_3), 0.9 (br, 1 H, CH_3), 1.65 (br, 2 H, CH_2), 3.59 (s, 8 H, OCH_2CH_2O), 3.4 (br, 14 H, $OCH_2CH_2O + OCH_3$), 4.05 (br, 4 H, $ArOCH_2$), 4.15 (br, 4 H, $ArOCH_2$), 4.6−4.9 (br, 2 H, Bz-H), 6.6−6.9 (br, 3 H, Ar−H), 7.14 (s, 2 H, Ar−H). ^{13}C NMR (75 MHz, $CDCl_3$, δ): 117.4, 167.7. 150.5, 148.9, 148.7, 128.3. 128.2, 125.4, 121.8, 114.5, 113.7, 113.3, 71.4, 71.2, 69.9, 69.6, 66.9, 52.5, 45.0, 29.7, 23.5. Anal. Calcd for $(C_{87}H_{110}O_{36})_n$: C, 59.81; H, 6.39. Found: C, 59.42; H, 6.71.

Poly(tetramethyl 16,16′-(16-(Methacryloyloxymethyl)-6,7,9, 10,12,13,20,21,23,24,26, 27-dodecahydrodibenzo[b,n][1,4,7,10,13, 16,19,22]octaoxacyclotetracosine-2,3-diyl) bis(methylene)bis-(oxy)bis(6,7,9,10,12,13,20,21,23,24,26,27-dodecahydrodibenzo[b,n]-[1,4,7,10,13,16,19,22]octaoxacyclotetracosine-2,3-dicarboxylate)) (***PG2***). Monomer **12** (300 mg) was dissolved in 0.3 mL of DMF at 30 °C, and 0.2 wt % freshly recrystallized AIBN was added. The solution was then placed in a preheated oil bath at 60 °C after careful degassing by three freeze−pump−thaw circles. After 72 h, the solution was cooled to room temperature and filtered over a short silica gel column with $CHCl_3$ as eluent. Yield: 70 mg (23%) of a colorless powder. ^{1}H NMR (300 MHz, $CDCl_3$, δ): 0.87 (br, weak), 1.94 (br), 3.5−4.3 (m, 72 H, OCH_2CH_2O; 12 H, $COOCH_3$), 4.8−5.0 (s, 4 H, Bz−H), 6.40 (br, 2 H, Ar−H), 6.47 (br, 2 H, Ar−H), 6.7−6.9 (br m, 5 H, Ar−H), 6.98 (br, 2 H, Ar−H), 7.15 (br, 4 H, Ar−H). ^{13}C NMR (75 MHz, $CDCl_3$, δ): 167.7, 153.8, 150.49, 150.48, 150.1, 148.8, 148.7, 143.4, 128.3, 125.4, 125.3, 115.7, 113.4, 133.3, 105.3, 102.9, 71.4, 71.2, 71.0, 70.3, 70.1, 69.8, 69.6, 69.1, 68.3, 52.5. Anal. Calcd for $(C_{87}H_{110}O_{36})_n$: C, 60.34; H, 6.40. Found: C, 60.43; H, 6.68.

Acknowledgment. We thank M. Colussi and T. Schweizer for all GPC and DSC measurements and A. Kägi and F. Messerschmitt for help with the NMR complexation studies.

Supporting Information Available: ^{1}H NMR and ^{13}C NMR spectra of all new compounds, crystal data of compound **3**, ^{1}H NMR (700 MHz) titration curve of **PG1**/KPF_6 and **PG2**/KPF_6 in CD_3CN, ^{1}H−^{19}F NOE correlation of **MG1**, **9**, **PG1**, and **PG2** complexed with excess KPF_6 in CD_3CN, and reduced scattering intensities of **PG1** in the LS-titration experiment with KPF_6 in acetonitrile. The crystallographic data information file is also provided. This material is available free of charge via the Internet at http://pubs.acs.org.

References and Notes

(1) Schlüter, A. D.; Rabe, J. P. *Angew. Chem., Int. Ed.* **2000**, *39*, 864–883.
(2) Schlüter, A. D. *Top. Curr. Chem.* **2005**, *245*, 151–191.
(3) Frauenrath, H. *Prog. Polym. Sci.* **2005**, *30*, 325–384.

(4) Zhang, A.; Zhang, B.; Wächtersbach, E.; Schmidt, M.; Schlüter, A. D. *Chem.—Eur. J.* **2003**, *24*, 6083–6092.
(5) Quali, N.; Mery, S.; Skoulios, A. *Macromolecules* **2000**, *33*, 6185–6193.
(6) Percec, V.; Ahn, C.-H.; Cho, W.-D.; Jamieson, A. M.; Kim, J.; Leman, T.; Schmidt, M.; Gerle, M.; Möller, M.; Prokhorova, S. A.; Sheiko, S. S.; Cheng, S. Z. D.; Zhang, A.; Ungar, G.; Yeardley, D. J. P. *J. Am. Chem. Soc.* **1998**, *120*, 8619–8631.
(7) Kim, H.-J.; Lee, E.; Park, H.-S.; Lee, M. *J. Am. Chem. Soc.* **2007**, *129*, 1994–1995.
(8) Percec, V.; Rudick, J. G.; Peterca, M.; Heiney, P. A. *J. Am. Chem. Soc.* **2008**, *130*, 7503–7508.
(9) Rudick, J. G.; Percec, V. *Acc. Chem. Res.* **2008**, *41*, 1641–1652.
(10) Pedersen, C. J. *J. Am. Chem. Soc.* **1967**, *89*, 7017–7036.
(11) Beginn, U.; Zipp, G.; Möller, M. *Adv. Mater.* **2000**, *12*, 510–513.
(12) Beginn, U.; Zipp, G.; Mourran, A.; Walther, P.; Möller, M. *Adv. Mater.* **2000**, *12*, 513–516.
(13) Percec, V.; Bera, T. K. *Tetrahedron* **2002**, *58*, 4031–4040.
(14) Percec, V.; Cho, W.-D.; Ungar, G.; Yeardley, D. J. P. *Chem.—Eur. J.* **2002**, *8*, 2011–2025.
(15) Gibson, H. B.; Yamaguchi, N.; Hamilton, L.; Jones, J. W. *J. Am. Chem. Soc.* **2002**, *124*, 4653–4665.
(16) Gibson, H. B.; Jones, J. W.; Bryant, W. S.; Bosman, A. W.; Janssen, R. A. J.; Meijer, E. W. *J. Org. Chem.* **2003**, *68*, 2385–2389.
(17) Buschbeck, R.; Lang, H. *J. Organomet. Chem.* **2005**, *690*, 696–703.
(18) Stoddart, J. F.; Leung, K. C.-F.; Aricó, F; Cantrill, S. J. *J. Am. Chem. Soc.* **2005**, *127*, 5808–5810.
(19) González, B.; Alonso, B.; Losada, J.; Garcia-Armada, M. P.; Casado, C. M. *Organometallics* **2006**, *25*, 3558–3561.
(20) Skobridis, K.; Alivertis, D.; Theodorou, V.; Paraskevopoulos, G. *Tetrahedron Lett.* **2007**, *48*, 4091–4095.
(21) Gibson, H. W.; Yamaguchi, N. *Macromol. Chem. Phys.* **2000**, *201*, 815–524.
(22) Alexandratos, S. D.; Stine, C. L. *React. Funct. Polym.* **2004**, *60*, 3–16.
(23) Calderón, V.; Schwarz, G.; Garcia, F.; Tapia, M. J.; Valente, A. J. M.; Burrows, H. D.; Garcia, J. M. *J. Polym. Sci., Part A: Polym. Chem.* **2006**, *44*, 6252–6269.
(24) Swager, T. M.; McQuade, D. T.; Pullen, A. E. *Chem. Rev.* **2000**, *100*, 2537–2574.
(25) Morina, K.; Kaptein, B.; Yashima, E. *Chirality* **2006**, *18*, 717–722.
(26) Yashima, E.; Miyagawa, T.; Yamamoto, M.; Muraki, R.; Onouchi, H. *J. Am. Chem. Soc.* **2007**, *129*, 3676–3682.
(27) Sakai, R.; Kakuchi, T. *Macromol. Symp.* **2007**, *249−250*, 81–85.
(28) Leung, K. C.-F.; Mendes, P. M.; Magonov, S. N.; Northrop, B. H.; Kim, S.; Patel, K.; Flood, A. H.; Tseng, H.-R.; Stoddart, J. F. *J. Am. Chem. Soc.* **2006**, *128*, 10707–10715.
(29) Although for the polyacetylene sample, an increase in the hydrodynamic radii from $R_h = 93$ nm for the uncomplexed polymer to $R_h = 98$ nm for the complex with a first generation dendron and to $R_h = 112$ nm for a third generation dendron was observed, these numbers should be interpreted with care. A polyacetylene chain of $DP_w = 33$ has a maximum length of only $L_w = 11$ nm, which renders R_h for the single polyacetylene chain to be certainly smaller than 5 nm. Apparently, the measured dimensions above 90 nm can be explained only by the formation of large aggregates. It is thus even more surprising that the authors succeeded in determining the molar mass of such aggregates utilizing the "molecular weight mode" of a Beckman Coulter N4 Plus PCS instrument, which agreed amazingly well with those determined by GPC and NMR ($M_w = 18.000$, 38.000, and 70.000 g/mol for the uncomplexed and complexed polymers with first and third generation dendrons, respectively.
(30) Hanson, I. R.; Hughes, D. L.; Truter, M. R. *J. Chem. Soc., Perkin Trans. II* **1976**, 972–976.
(31) Burchard, W. *Polymer* **1969**, *10*, 29.
(32) Förster, S.; Schmidt, M. *Adv. Polym. Sci.* **1995**, *120*, 51–133.
(33) Rapp, A.; Schnell, I.; Sebastiani, D.; Brown, S. P.; Percec, V.; Spiess, H. W. *J. Am. Chem. Soc.* **2003**, *125*, 13284–13297.
(34) Holzberger, A.; Kleinpeter, E. *Magn. Reson. Chem.* **2004**, *42*, 589–593.
(35) Wacker, P.; Kleinpeter, E. *J. Inclusion Phenom. Mol. Recognit. Chem.* **2007**, *59*, 331–339.
(36) Loh, P. Dissertation, Mainz, Germany, 2008.
(37) Loh, P.; Deen, G. R.; Vollmer, D.; Fischer, K.; Schmidt, M.; Kundagrami, A.; Muthukumar, M. *Macromolecules* **2008**, *41*, 9352–9358.
(38) Kratky, O.; Porod, G. *Recl. Trav. Chim. Pays−Bas* **1949**, *68*, 1106.
(39) Schmidt, M.; Stockmayer, W. H. *Macromolecules* **1984**, *17*, 509–514.
(40) Oberthür, R. C. *Macromol. Chem. Phys.* **1978**, *179*, 2693–2706.
(41) Engelkamp, H.; Middelbeek, S.; Nolte, R. J. M. *Science* **1999**, *284*, 785–788.
(42) He, G.-X.; Imato, T.; Ishibashi, N.; Shinkai, S.; Matsuda, T. *Bull. Chem. Soc. Jpn.* **1990**, *63*, 401–406.
(43) Eliasson, B.; Larsson, K. M.; Kowalewski, J. *J. Phys. Chem.* **1985**, *89*, 258–261.
(44) Buchanan, G. W.; Moghimi, A.; Ratcliff, C. I. *Can. J. Chem.* **1996**, *74*, 1437–1446.
(45) Erk, C.; Zeidler, M. D. *J. Mol. Liq.* **1999**, *79*, 17–26.
(46) Ameijde, J. v.; Liskamp, R. M. J. *Org. Biomol. Chem.* **2003**, *1*, 2661–266.
(47) Anderson, D. R.; Koch, T H. *J. Org. Chem.* **1978**, *43*, 2726–2728.
(48) Cantrill, S. J.; Youn, G. J.; Stoddart, J. F. *J. Org. Chem.* **2001**, *66*, 6857–6872.
(49) Becker, A.; Köhler, W.; Müller, B. *Ber. Bunsen−Ges.* **1995**, *99*, 600.